



Appendix 3 – Characterization of sediment plumes behind mining vehicles in the NORI area

Characterization of sediment plumes behind mining vehicles in the NORI area (laboratory analyses)

Authors: Benjamin Gillard and Laurenz Thomsen

iSeaMC@OceanLab

Bremen, 11.11-2020

5th draft

Summary

- Sediments from the Nori-D site for aggregation experiments and Type 1 nodules for experiments on blanketing were delivered by DG, AllSeas and BF. A test section for a seawater flume was prepared for the nodules using original sediments.
- Two flow conditions were simulated: 3.5-4 cm/s average flow velocity at the mining site (resembling a shear rate of ≈ 0.1 G), and 15 cm/s (flow velocity of an eddy passing through the mining site under 1G).

Results

- Plume dispersal in the near-field area with concentrations of 1 – 10 g/l dw (≈ 40 g/l sediment wet weight) of sediments (0-15 cm) under elevated (1G, 15 cm/s) and normal (0.1 G, ≈ 4 cm/s) turbulence results in rapid aggregation of deep sea sediments after they passed through the high-shear collector pump .
- As expected by theoretical and empirical studies on aggregation, the process starts immediately. Under both concentrations, larger particles with median sizes (d_{50}) of ≈ 700 μm (0.1G) and ≈ 2000 μm (1G) are formed within the first 30 minutes while particle fallout takes place simultaneously.
- For both scenarios, a rapid export phase of the aggregates lasts for around 120 min and particle concentrations drop well below 10 % of the original concentration.
- Constant release of plumes particles will extend that export phase over hours to days, while the “Core aggregation” phase towards large aggregates remains fast but will also constantly take place.
- Settling velocities of individual aggregates in stagnant waters of a settling column under these elevated plume concentrations varied between 62 and 705 m/day. **These results can be used for particles settling at a midwater point , in the water column (1000-4000 m)or well above a fluid mud layer in the benthic boundary layer.**

For the fluid mud layer which develops behind the collector we also applied another approach to better understand the behavior of concentrated plume injections $\geq 1\text{g/L}$ to determine effective settling velocities under hindered settling (see below). For that we used the data from an Aqualogger turbidity meter, which automatically adapts to increasing particle concentrations. The calculated settling velocities were much lower for a floc population, which was exposed to both, hindered settling and turbulence. This behavior can be expected in highly concentrated plumes.

- Under averaged settling velocities of 0.013 cm/s for floc populations developing under plume concentrations of 10 g/L, these particles can be transported over tens of kilometers under the conditions of hindered settling.
- During mining operations with constant plume release a fluid mud layer is formed from “hindered settling” which consists of un-consolidated loose aggregates which should easily form a gravity flow. This fluid mud layer is compacted and consolidated over time but remains unstable and loose as long as particles settle into it.
- Once the plume release is stopped, the fluid mud layer is compacted and decreases its thickness within hours.
- Type 1 nodules are easily blanketed by this consolidated mud layer and in the far field area with particle concentrations $< 1500\text{g/L}$ a linear relationship between blanketing thickness, sediment load and particle concentration was determined which allows DG to estimate blanketing under different scenarios of plume concentrations and duration. For the near field area a scenario was developed for $> 10\text{g/L}$ deposition.
- For the near filed scenario with particle concentrations between 1 and > 10 g/l the accumulating blanketing layer will be further compacted and consolidated by its increasing mass.
- Under higher plume concentrations of 10 g/l fine particles not scavenged by the aggregation process remain in the water column for days. When they reach the seafloor without being scavenged by larger aggregates, they form a very fine powder-like cohesive top-layer of the blanketing.

- Once Type 1 nodules are completely blanketed, this layer prevents resuspension up to flow velocities of 15 cm/s and creates a new sediment surface at the exploration site.

I. Overview

The dispersal of a sediment plume during mining operations poses the biggest impact for the deep sea environment. A reliable forecast of the fallout areas of the generated plume is important and reliable data on the behavior of plume particles are therefore essential. Following the discussion with Deep Green we hereby report data and recommendations from laboratory studies with original sediments from the NORI exploration site.

Depending on the hydrodynamic conditions and aggregation potential of the sediment plume, aggregates of different particle sizes will settle at variables speeds and distances from the source and will deposit on the sea floor. Over time, this deposition will cause a complete coverage (blanketing) of the seafloor and most of the associated fauna.

So far, this blanketing effect has only been qualitatively investigated in small disturbance experiments on the basis of image analyses of the sea floor, without quantitative data on the relation of microtopography of the manganese nodules with the associated hydrodynamics environment. The aim of this contract is therefore to gain more precise knowledge using in-situ samples. Four scenarios were investigated which lead to blanketing effects.

- A. A scenario right behind the collector with a concentration ~ 10 g/L, at an average shear rate of 1 s^{-1}
- B. A scenario right after a reinjection with a concentration ~ 10 g/L, at a shear rate of 0.1 s^{-1} .
- C. A scenario in the middle of the plume with a concentration ~ 1 g/L, at a shear rate of 0.1 s^{-1}
- D. A scenario of remaining background plume, when most of the aggregation had taken place with a concentration ~ 30 mg/L, at a shear rate of 0.1 s^{-1} .

Approach and boundary conditions

The results should describe the characteristics of a plume at three different locations around a mining vehicle and at the reinjection point at midwater depth. Concentrations are given in g dry weight per liter.

Shear rates ($G \text{ s}^{-1}$) were corresponding to free stream velocities of

- A: $0.1G \approx 3.5\text{-}4 \text{ cm/s}$ (average flow velocity at the mining site; $u_* \approx 0.2 \text{ cm/s}$);
- B: $1G \approx 15 \text{ cm/s}$ (flow velocity of an eddy passing through the mining site; $u_* \approx 0.9 \text{ cm/s}$)

Experiments were carried out at salinities of 35 and ambient temperatures of $2\text{-}6^\circ \text{C}$.

2. Methods

Aim of this study is to simulate a dispersal of sediment plumes of three different particle concentrations (0.03, 1, 10 g/L dry weight) into the benthic boundary layer at the NORI site. For the process of aggregation

and to produce enough material for flume experiments with manganese nodules we use a water column simulator (Sanford, 1997). For experiments on blanketing and erosion under different flow conditions a seawater flume is used (Garcia & Thomsen, 2008). Experiments were run in triplicates.

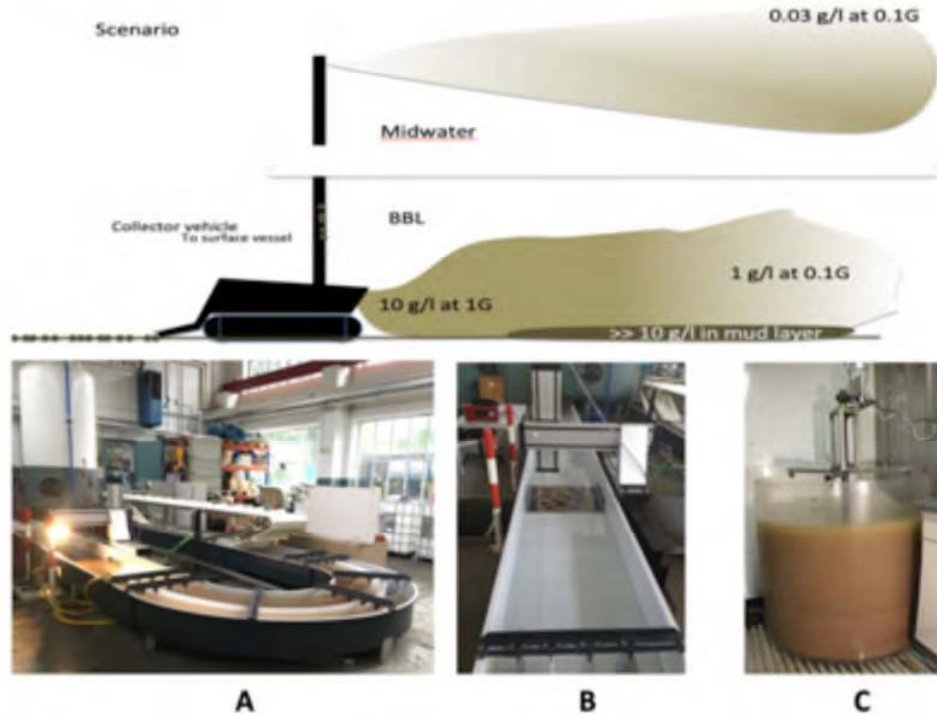


Fig.1. A,B: Seawater flume (16 m) with 0.25 m² test section; C: Water column simulator (1000 l)

Arrival of samples

MUC samples without nodules were sent from BlueField and arrived April 15. 310 kg of boxcorer samples from AllSeas arrived on Wednesday, May 6 together with 110 kg of manganese nodules. Samples were stored in a cool room at $\approx 3^{\circ}\text{C}$. Experiments and analyses started, after the temperature of the sediments had reached those of the cool room. The project report was due 3 months after arrival of sediments and nodules.

Selection of samples

Polymetallic nodules from the CCFZ NORI site were used to represent a typical exploration site of ≈ 16 kg wet weight. Type 1 nodules representing 90 % of samples taken from the NORI – D site were used. These Type – 1 nodules are unimodal and tightly dispersed around a mean of 2 – 3 cm. A figure with the typical size distribution of Type 1 nodules from a “2019 resource update” was provided by Anthony O’Sullivan on June 9. From the nodules provided by AllSeas on May 6, a total of 286 nodules (≈ 90 % of all fully intact nodules in the 110 kg sample) were selected carefully to generate a similar size distribution and placed in a 0.12 m² box prepared with original sediments (Fig.4). Each nodule was placed into the sediment with the correct side up (hydrogenic nodule growth side) and embedded down to the mark showing the sediment water interface. The sample, hereafter called “Type1 nodules” were then transferred into the test-section of the flume (Fig.5).

The following sediments were then separated for analyses: BC-094 and BC-110 which represent Type 1 nodule sediments and BC-124 representing Type 3 nodules. Only triplicate sediment samples from the top layer (0 - 15 cm) were analyzed. Those characterize sediments removed during mining operation. For the experiments we needed tens of kg of (near) surface sediments from stations with type 1 nodules. 0- 5 cm sediments from other stations were available but not at that amount.

2.1. Analysis of plume behavior

Particle sizes analysis

A modified combined approach using a LISST-100X (Laser In-Situ Scattering and Transmissometry, Sequoia Scientific) coupled with an industrial camera (DFK 23UX174, The Imaging Source) mounted with a telecentric lens (TEC-M55MPW, Computar) (Fig.1) was used to determine the sediment particle sizes (Mikkelsen *et al.*, 2005; P.S. Hill *et al.*, 2013). When combined with a particle camera, this set up allowed to detect a broad range of particle sizes ranging from 2.5 microns up to couples of millimeters (Gillard *et al.*, 2019).

Step 1: Particle size and composition

Sediments from the 3 different NORI sites were disaggregated and analyzed for the particle size distribution. Particle size analyses were performed according to Gillard *et al.*, 2019. As results of the particle size distribution showed normal abyssal plain sediments of the CCZ without larger biogenic compounds (Gillard *et al.*, 2019), no further microscopic analyses were carried out.

Step 2: Particle size behind the collector

Sediments from representative NORI box corers BC-094, BC-110 (Type 1 nodules) and BC-124 (type 3 nodules) were disaggregated using a strong centrifugal pump (3000 RPM) to simulate the transport through the collector under high shear.

Aggregation processes

Introduction to aggregation. Collision between suspended particles depends on the size/settling velocity distribution of the particles and on the movement of the water. In the water column, turbulence and differences between the settling velocities of particles are the dominant control on aggregation rates, which consist of three main processes. Firstly, particles must be brought into close proximity, a process named 'encounter. Secondly, these particles must be brought into direct contact by the flow fields around them, a process called 'contact. Finally, the particles must 'stick together. The encounter rate is a function of particle size, settling velocity and turbulence, whereas contact and stickiness are efficiencies related to relative particle size and physicochemical properties of particles, respectively (Thomsen & McCave, 2000). Aggregation and disaggregation process of particulate matter occur continuously in the ocean.

Step 3: Aggregation

Aggregation due to turbulent shear

The water column simulator consists of an inner paddles slowly rotating in a cylinder (110 cm diameter), based on the design of Sanford (1997) at a temperature of 2.0 °C. Shear rates of 0.1 and 1 G (s^{-1}) typically found in the BBL at the CCFZ under normal condition (0.1 G) and during the transition of an eddy (1G) or

behind a mining vehicle were simulated. A turbidity sensor (Aqualogger 310TY, Aquatec) able to reach maximum concentrations of 40 g/L (d.w.) was calibrated using the BC sediments provided by DG and used for particle concentration. A total of 200 to 2500 particles were analyzed semi-automatically for each experimental setup on aggregation and particle size distribution, using the program Image-J (<https://imagej.nih.gov>).



Fig. 2. Experimental setup in cool-room and water column simulator with developing mud layer

Step 4: Settling velocities

The aggregate size vs. settling velocity relationship is determined using a temperature-controlled settling column developed by Gillard et al., 2019. The column is designed to be operational under constant temperature (cooling system) and able to be mounted and on the LISST-100X for fine particle settling speed determination. The particles are 360° up-illuminated and settling rates vs. particle sizes are determined with a high-resolution camera. The post processing method is applied using the software ImageJ (<https://imagej.nih.gov>) which allows to investigate the settling speed and trajectory dynamics (Fig. 3B) of hundreds of aggregates at microscale definition. Settling velocities were analyzed under increasing plume concentrations to estimate the importance of hindered settling with the subsequent generation of a fluid mud which would generate a gravity current under slope angles of $> 1^\circ$.

Data processing for evolution of D50 aggregate size over time.

All analyses were carried on using MATLAB 2019b.

The grid of the X axis (time) was made in 1 min step intervals (240 in total).

1D cubic spline interpolation was used to fit the dataset, using not-a-knot end conditions. The interpolated value at a query point is based on a cubic interpolation of the values at neighboring grid points in each respective dimension.

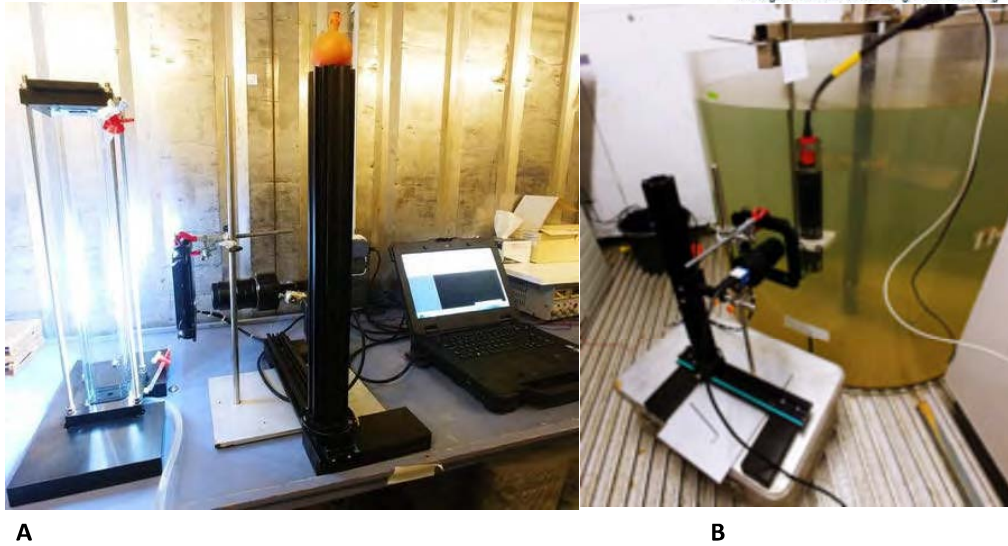


Fig.3. Settling column (A), and particle camera (B) in the coolroom

Step 5: Blanketing effect generated by a settling sediment plume

The thickness of a blanketing layer was investigated using the large seawater flume (Fig.1C).



Fig.4. Test section, with 286 Type 1 nodules from the NORI exploration site (≈ 16 kg ww)

The blanketing layer thickness and 3D structures formed under 5 different scenarios are analyzed:

1. under 10 g/L plume concentrations at 1G in the water column (near field)

2. under 1 g/L plume concentration at 0.1 G in the water column (near field)
3. under ≈ 0.03 g/L plume concentration in a 50 m water column (far field) or re-injection point
4. under 0.01 g/L plume concentration in a 50 m water column (far field)
5. under 0.01 g/L plume concentration in a 25 m water column (far field)

After blanketing experiments a 3D scanner provided analyses on the thickness and structure of the settled plume on the manganese nodules. Samples from the mud layer were collected and stored in a cool room and could be sent to Deep Green on demand for further analyses of the new sediment properties.

D. Topography and flow field measurements

The measurements of topography and flow field were made using an ADV Vectrino profiler (Nortek, R. G. A. Craig et al., 2011) mounted on a 3D arm (Isel) for precise location of each measuring points (Fig. 5). Measurements were carried on the Typ1 nodule sample and after the blanketing experiment to allow a quantitative analysis of the sediment thickness as well as the flow field variation once the plume had settled.

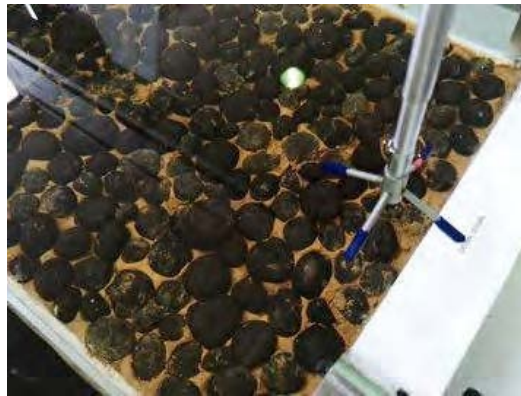


Fig. 5. Nortek Vectrino ADV profiler view into the test section of the flume

The micro-topography was mapped with the bottom detection capability of the instrument (10 Hz) and the Vectrino plus software (Nortek). MATLAB 2019b was used to compile the data and producing a first 3D mesh grid. This 3D mesh was further imported in MeshLab (www.meshlab.net, P. Cignoni *et al.*, 2008) for post-processing and texture layering. Overall, the measuring mesh grid was created from approximately 200,500 data points (6 hours per profile). The comparison between the original and blanketed sample was obtained using a 3D point cloud processing software CloudCompare (www.danielgm.net/cc).

Flow field measurements (200 Hz) were directly triggered by the Isel arm once it reached its measuring position. A grid resolution set to 6 mm in the XY direction and 7 mm in the Z direction was chosen for the ADV (signal to noise ratio) and overall profiling time (3 hours per layer profiled). In total, 5 layers above the nodule field were analysed. Overall, the 3D flow field mesh grid was created from approximately 13,500 measuring points. All datasets were transferred to Paraview software (www.paraview.org, A. James *et al.*, 2005) which allow the visualization of combined topography and flow field measurements.

Step 6 Resuspension behavior of the blanketing layer under different flow conditions

The critical erosion velocity of plume sediments blanketing a nodule layer were analyzed. For that the plume

layer remained on the nodules under typical low flow velocities of 0.1 G (3.5 cm/s) for 4 hours and checked after 24 hours. Then the flow velocity was subsequently increased to 1 G flow (15 cm/s, passing eddy) to determine bedload transport and suspended-load transport. Photos and videos will be provided and analyzed. The approach is similar to the method published by Thomsen and Gust (2000).

Explanation-videos, photographs, processed data for the figures and tables will be transferred as supplementary materials onto a server provided by DG and available for download by September 15.

2. Results

A. Size distribution of disaggregated deep-sea sediments

The sediments samples (0-15 cm mixtures of the box cores BC-094, BC-110 and BC-124) were used for the experiments since they were available in larger amounts compared to MC samples provided by BlueField. The particle size distribution indicates that median particle size (d_{50}) was 12 μm , with the 25 % percentile at 3-4 μm , and 75 % percentile located at 26-29 μm and presented in the Fig. 6. Please note that these results do not necessarily resemble surface sediments, since they are a mix of the top 15 cm from these sites. Median particle size in these top 15 cm of sediments was lower than those from other sites at the BGR CCFZ ($D_{50} > 20 \mu\text{m}$, published) but similar to other parts of the BGR and Belgian sectors (D_{50} of around 8-25 μm).

Dry solid density of the sediments is expected to be $\approx 2400 \text{ kg/m}^3$ and a d_{50} of only 12 μm , with a bulk wet density of the upper 10 cm of sediments of $\approx 1230 \text{ kg/m}^3$.

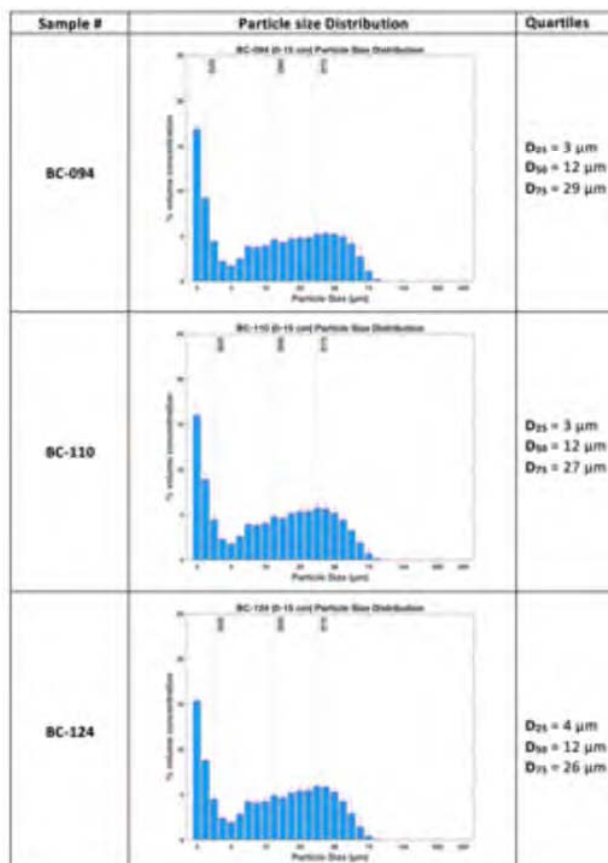


Fig. 6. Particle size distribution of NORI sediments used in this study.

B. Aggregation of 1 g/L sediment plume at a shear rate of 0.1 G (0.1 s^{-1} , $\approx 4\text{cm/s}$ flow velocity)

The Fig. 7 presents the conditions during the first 4 hours within a concentrated plume in a 1 m water column under shear rates of 0.1 s^{-1} . Three main flocculation phases could be identified (Gillard et al., in prep): the core aggregation, the export, the late aggregation.

The core aggregation phase 1 starts immediately after the plume is released. Within 30 min large aggregates are formed (confirming the result from Gillard et al., 2019). During that time, the size distribution of primary particles of d_{50} of $12 \mu\text{m}$ (Fig.6) rapidly shifts towards large aggregates with d_{50} of $680 \mu\text{m}$ (Fig. 7 I, blue line, d_{75} of $> 1000 \mu\text{m}$, pink area). This phase of constantly growing aggregates appears during the first 30 min (Fig. 7 I) and would continue during a permanent release of a plume, while simultaneously these particles are settling (exported) towards the seafloor. During this time, an export of $\approx 50 \%$ of the initial plume concentration) down to $\approx 450 \text{ mg/L}$ can be seen (Fig. 7 III, IV). Note that figures 7 III, A-F show the vertical particle concentration profiles within the 1 m water column, while Fig. 7 IV shows the change of particle concentration at 50 cm water depth (mid height of the water column simulator).

Phase 2, the export phase is characterized by decreasing aggregate sizes (Fig.7 I) and occurs between 30 and 120 min, as showed in fig. 7 I. During that phase, when particle numbers (indicated by particle concentrations) needed for aggregation rapidly decrease as a result of the fallout of large aggregates, the d_{50} of newly formed aggregates decrease from $680 \mu\text{m}$ to $280 \mu\text{m}$ while almost 90 % of the plume has settled to the bottom of the water column simulator after 60 minutes. This outcome shows that aggregates created at one concentration will change their size with a decrease in concentration even when the mixing conditions remain constant. The duration of the export phase (120 min in this case) which already starts immediately after plume release via aggregation and subsequent fallout is dependent on the water column height. A constant release of additional plume water would extend this core phase, however after a stop of such a release the export phase would occur in a similar time frame. In the case of this experiment after 120 min the overall plume concentration dropped to 72 mg/L .

The late aggregation phase spreads from 120 min onward. During that time the plume export slows down as the remaining particle concentrations in the water column have drastically decreased. At the end of the experiment (4 hours), the particle concentrations in the plume had been reduced from 1000 mg/L at the release to $\approx 50 \text{ mg/L}$. Even after 24 hours, the analysis of the remaining suspended particles indicates the presence of aggregates $> 200 \mu\text{m}$ (Fig 7 II) and the d_{50} is expected to increase again as a result of additional aggregation (see. Gillard et al., 2019 for details under low plume concentrations of $< 200 \text{ mg/L}$). Those aggregates have been created over a long period under the remaining low plume particle concentrations. They have scavenged more of the fine fraction $< 200 \mu\text{m}$ (Fig.7 II, at 1440 min, indicated by blue color) and can be exported over larger distances under the low turbulence of 0.1 G.

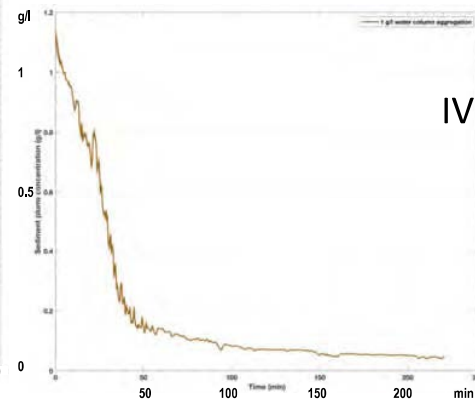
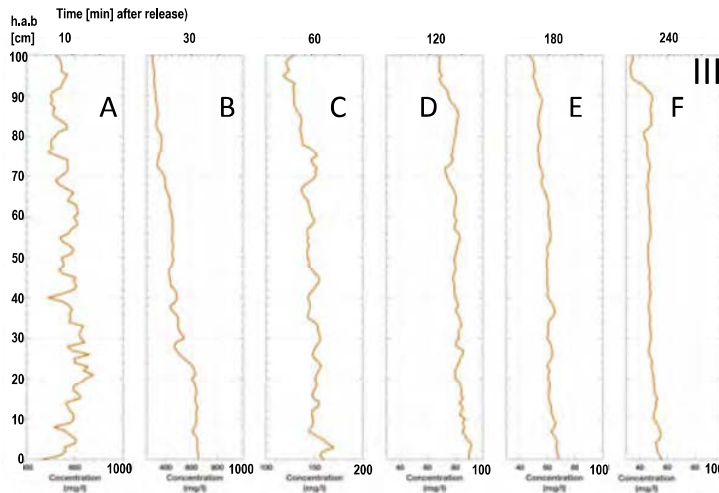
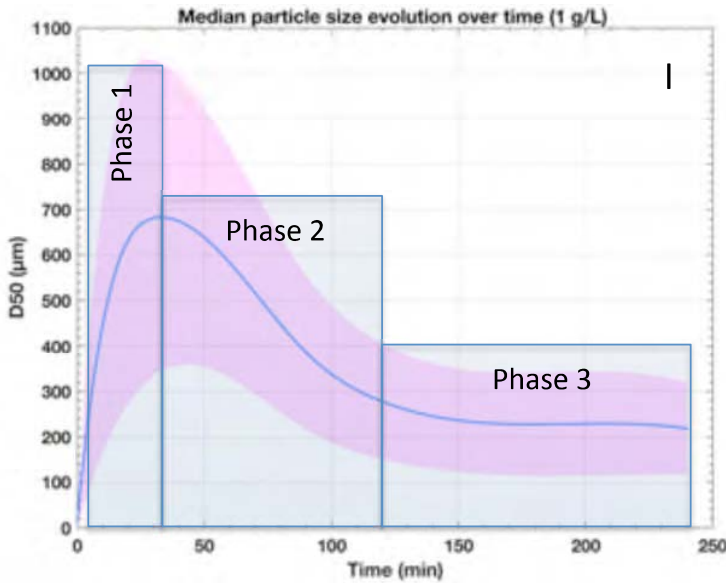
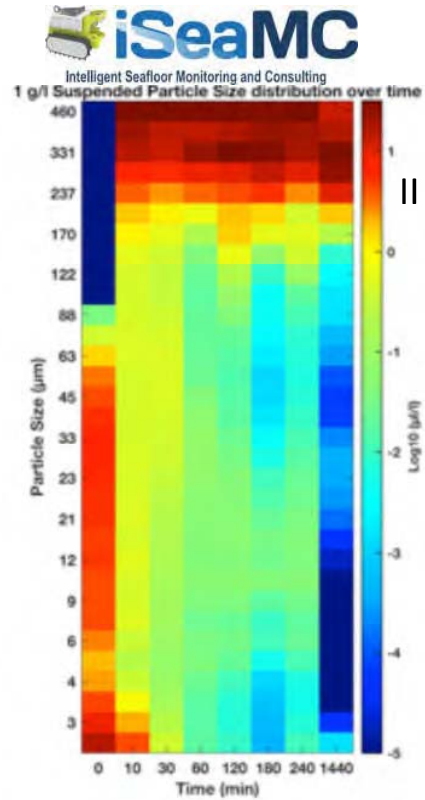


Fig. 7. Sediment plume aggregation dynamics at 0.1 G under 1g/L in the water column simulator. I: d_{50} (blue line) \pm STD (pink area) from particle camera data, analyzed with Matlab; II: determined by the LISST laser sizer at mid-height; III, IV: determined with Aqualogger turbidity meter (vertical profile run, run with Aqualogger at mid height)

C. Aggregation of 10 g/L sediment plume at a shear rate of 1 G (1 s^{-1} , $\approx 15 \text{ cm/s}$ flow velocity)

The Fig. 8 presents the conditions during the first 4 hours within a concentrated plume of 10 g/L in a 1 m water column under shear rates of 1 s^{-1} . Under these 10x higher plume concentrations and higher turbulence, within 30 min after release the core aggregation phase results in large aggregates with d_{50} of 1900 μm (Fig. 8 I, blue line, d_{75} of $> 2700 \mu\text{m}$, pink area), while simultaneously these particles are rapidly settling (exported) towards the seafloor. Already after 30 minutes a mud layer of a few centimeter height with particle concentration $\leq 20 \text{ g/L}$ begins to form (Fig 8 III). Within the main export phase (30 – 120 min after release) of decreasing aggregate sizes (Fig.8 IB) the d_{50} of newly formed aggregates decrease from 1900

µm to 300 µm while an almost 20 cm thick mud layer of unconsolidated particles of < 35 g/L has been formed (Fig. 18 III)

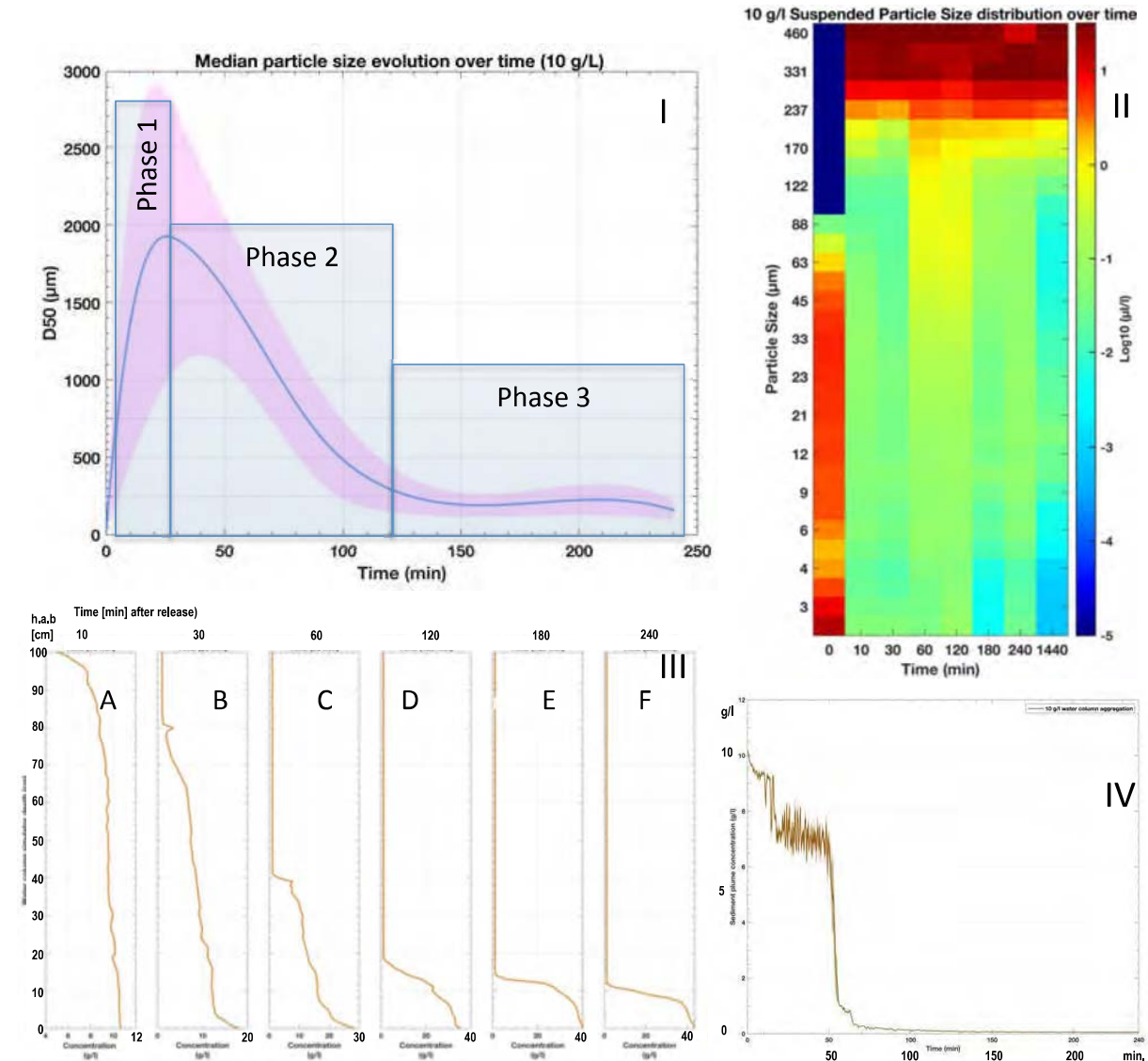


Fig. 8. Sediment plume aggregation dynamics at 1 G under 10g/L in the water column simulator. I: d_{50} (blue line) \pm STD (pink area) from particle camera data, analyzed with Matlab; II: determined by the LISST laser sizer at mid-height; III, IV: determined with Aqualogger turbidity meter (vertical profile run, run with Aqualogger at mid height)

The duration of the full export which already starts immediately after plume release via aggregation and subsequent fallout is dependent on the water column height. After 60 min, the overall plume concentration above the mud layer dropped below 10 % of the initial concentration of 10 g/L and is then expected to follow the process described for plume concentrations of 1 g/L but under higher turbulence. In fact, after additional 60 minutes the particle concentrations had dropped by another 90 %, following the behavior of the plume deposition of under 1 g/L. 240 min after the release of the plume a 10 cm thick and compacted mud layer with particle concentrations of 35 – 40 g/L (Fig. 8 III) has formed. Aggregates remaining in the water column resemble those detected under conditions of 1 g/L release in terms of particle size and volume

(Fig.7 II , 8 II, Log10 [µl/l]). Throughout the concentration drop under the two different initial plume concentrations, there is little difference between the aggregate sizes at a particular concentration, e.g., 100 mg/L. Since the main export phase ends already after 60 min when ≥ 90 % of the particles have settled at 10 g/L we used the 1 g/L at 0.1 G for interpretation of the 10 g/L scenario at 0.1 G. We then started additional experiments on hindered settling.

D. Settling velocities of individual plume aggregates in the settling column [w_s]

Curve fitted settling velocity (after Gillard et al., 2019)

Statistical analysis

The particle size and settling velocity datasets were first cleaned of extreme outliers (i.e. values higher / lower than 1.5 interquartile ranges above / below the 0.75 / 0.25 quartiles, respectively) and grouped by sediment concentration and by shear rate. Since particle sizes differed among the different groups, the measured velocities were normalized to the median particle size.

Modeling of settling velocities

A non-linear (logistic-sigmoidal) curve was fitted to model settling velocity against particle size for each concentration-shear rate combination, and 95 % confidence and prediction intervals were calculated based on each model. The curves followed:

$$y = \frac{a_1}{1 + e^{\frac{a_2 - x}{a_3}}}$$

where a₁ was the upper asymptotic limit of the curve, a₂ was the inflection point of the curve and a₃ a scaling factor for the size axis.

Modeled settling velocities for aggregates produced under 1 (A) and 10 (B) g/L

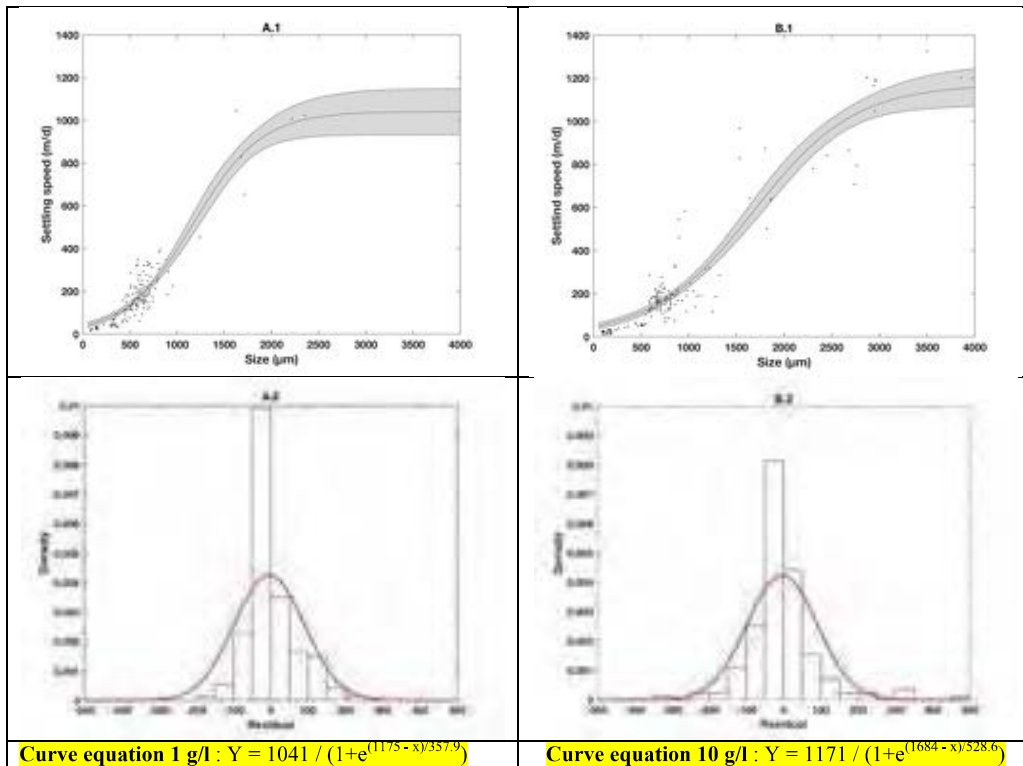


Fig. 9. Fitted model equation of settling velocities from deep sea sediment plume aggregates. Combined raw data and predicted model curve with corresponding 95 % confidence interval of aggregates produce under sediment plumes of (A.1) 1 g l⁻¹ under 0.1 G; (B.1) 10 g l⁻¹ under 1 G. Bottom line model residual histogram with plotted normal curve distribution.

Modeled settling velocities for aggregates produced under 1 g/L at 0.1 G (A) and 10 g/L at 1 G (B) with regression line

The two-regression lines presented in the figure below are equivalent to the regression line proposed for Deep-Green draft report figure 9. Figure A.1 correspond to 1 g/l experiment and B.1 to 10 g/l experiment.

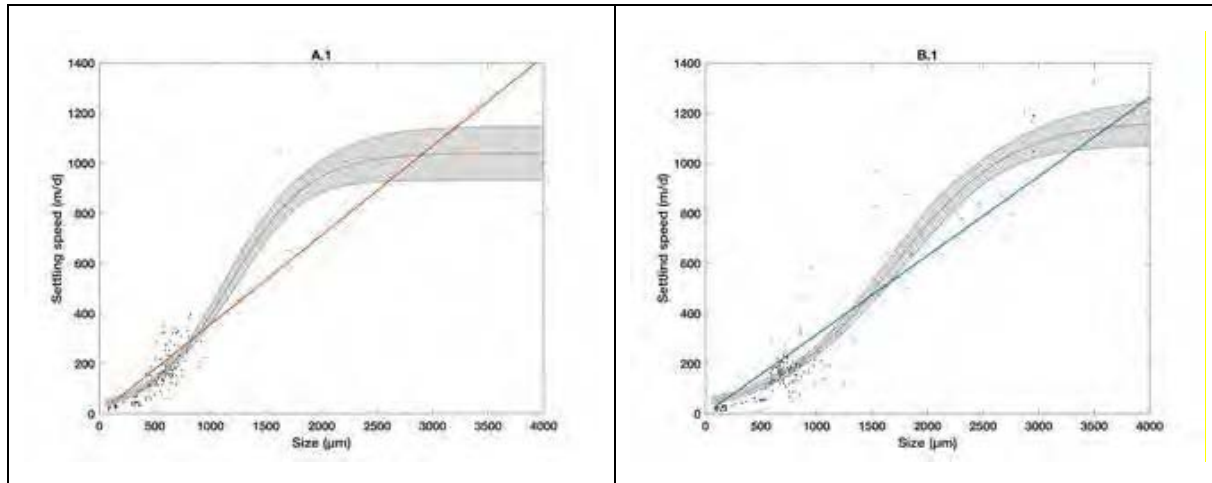


Fig. 10. Comparison with data from draft report (07.09.2020), where a linear relationship between size and settling velocity was calculated.

Comparison of settling velocity with Gillard *et al.* 2019

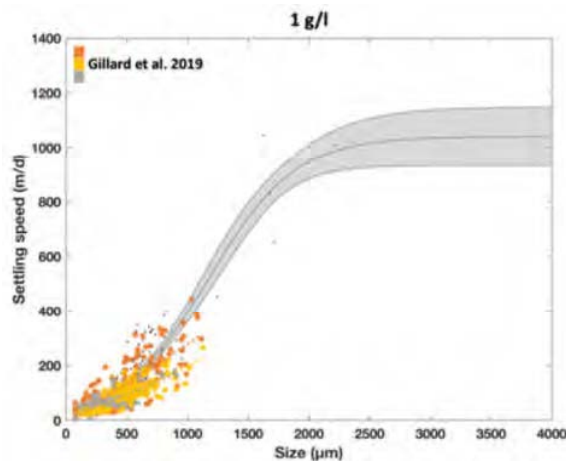


Fig. 11. Comparison with Gillard *et al.* 2019 data from BGR. Orange: 105 mg/L

Based on the observation that the d_{50} of BGR sediment was bigger than Deep green sediment, for equal shear rate and aggregate size, more particles will be incorporated into aggregates at the NORI site. This will result in denser particles of higher settling velocities.

Calculated specific settling velocities, typically expected at a midwater injection point with elevated turbulence

W_s at 1 g/L

The calculated settling velocities of aggregates at different times of the experiments (phases 1 – 3, see Fig. 7) varied for the d_{50} size between 67 and 209 m/d (Fig. 9). As expected, W_s increased during the first 30 minutes when aggregate size increased during the “core aggregation” phase. Between 60 and 120 min after release of the plume, when > 90 % of the flocs had already settled through the 1 m thick water column, both aggregate size and corresponding settling velocities decreased accordingly. However, after 24 hours size median floc size and settling velocity had increased again. This is the result of an ongoing aggregation process in phase 3 (late aggregation), when large aggregates are still in suspension and scavenge the still existing fine fraction in the water column.

It is worth pointing out that the aggregates formed during the “core aggregation phase” (phase I in fig. 7, 8) during the first 30 minutes might not follow the trend in size/settling velocity relationship between 30 to 240 minutes. Smaller aggregates are characterized by lower settling velocities and follow the lower end of the curved d/w_s relationship shown in figure 10. This behavior was also visible in other studies (see Fig. 4 of Gillard et al., 2019). Thus there is obviously a difference in the d/w_s relationship during the initial aggregation process (phase I) when compared to the export phase (phase II), when aggregates had reached a maximum size under the given conditions of turbulence and particle concentration and settle out.

Settling also occurs already during phase I but the process of larger aggregate formation obviously results in comparably lower settling velocities. This is possibly the result of compaction and subsequent increase in excess density of the aggregates during an increasing encounter rate; but more likely the increasing scavenging rate of the porous aggregates. Larger particles can be much more important in scavenging smaller ones if they are porous (Stolzenbach, 1993) and if they entrain small particles into their wakes as they settle (Hill and Nowell, 1990), as these mechanisms increase the collision efficiency. Thus with each scavenging process of larger aggregates which settle faster or collide with the very fine original sediments (d_{50} of 12 μm at the NORI site), the excess density of the aggregates increases which results in elevated settling velocities. This however should be further investigated but should not concern DHI, since you are mainly interested in phase II and III (Fig. 7,8) to simulate an ongoing plume injection. For modeling purposes DHI should focus the export phase only, when the newly formed aggregates do not grow in size any more but settle out while scavenging the remaining fine fraction of the initial fine fraction of $d_{50} = 12 \mu\text{m}$.

W_s at 10 g/L

At 10 g/l initial plume concentration the settling velocities of individual aggregates in the settling column at different times of the experiments (phases 1 – 3, see Fig. 8) varied for the d_{50} sizes between 62 and 705 m/d. The same trend in W_s during the first 30 minutes was detected when aggregate size increased during the “core aggregation” phase. Again, after 24 hours the median floc size and settling velocity increased again, when even more large aggregates were still in suspension and scavenged the still existing fine fraction in the water column (see also Fig 8, II).

These results must however be interpreted with caution, especially when intended to use for particle transport models under high plume concentrations !

Table 1A. Size distribution and corresponding calculated specific settling velocities of individual aggregates of decreasing plume concentrations from initially 1 g/L over time (T) in minutes. See numbers in brackets [1], [2] to compare similar sized aggregates

		1 g/L						
Unit		T=10	T=30	T=60	T=120	T=180	T=240	T= 24h
Particle Concentration [g/L]		0.911	0.427	0.140	0.072	0.053	0.046	0.008
d ₂₅	µm	294	465[1]	279	199	161	154	282
d ₅₀		448[1]	681	386	278	228	218	326
d ₇₅		671[2]	933	506	370	313	289	375
Ws ₂₅	m/d	81.8	125.9[1]	78.7	63.9	57.8	56.7	79.3
Ws ₅₀		120.7[1]	209.2	103.4	78.5	68.9	67.2	88.8
Ws ₇₅		204.6[2]	350.9	139.1	99.3	85.9	80.8	100.6

Table 1B. Size distribution and corresponding calculated specific settling velocities of individual aggregates at decreasing plume concentrations from initially 10 g/L over time (T) in minutes. Note that these results show the behavior of particles above a fluid mud layer.

		10 g/L						
Unit		T=10	T=30	T=60	T=120	T=180	T=240	T= 24h
Particle Concentration [g/L]		9.368	6.559	0.767	0.079	0.058	0.052	0.007
d ₂₅	µm	863	1292	430[1]	213	157	122	318
d ₅₀		1378	1902	641[2]	296	206	161	371
d ₇₅		2085	2395	830	412	268	208	437[1]
Ws ₂₅	m/d	204.5	377.8	99.9[1]	68.2	61.7	58.0	82.2
Ws ₅₀		420.6	704.6	142.9[2]	79.0	67.4	62.2	90.2
Ws ₇₅		797.5	929.0	194.2	96.8	75.2	67.6	101.1[1]

After ≈ 120 minutes, when most of the particle fallout had taken place under different initial particle concentrations, subsequent settling velocities of both particle groups were similar.

These settling velocities should be used for particles settling above the fluid mud layer or at a midwater injection point.

The particle concentrations of 0.007 and 0.008 g/L after 24 hours of aggregation and subsequent export are low. The increase of aggregate size between 3 and 24 hours after injection can however be considered as a relevant process during the settling of the remaining aggregates through a water column even at such low particle concentrations. The particle concentrations for the CCZ in the lowermost 10 m water column are in the order of < 100 µg/L (Gardner et al., 2018). For midwater conditions there are very few data available but own results from particle camera deployment show particle numbers around 100 - 300 particles /L, which can be a few hundred µm in size (Gillard, in prep). Aggregate studies at continental margins at 4000 m depth revealed particle concentrations in the BBL of ≈ 3 mg/L, with aggregates of d_{50} of 300 µm and N of 200 – 300/L. Under these particle concentrations scavenging of 10 µm particles is unlikely, especially when the larger particles are low in organic content. However, an incoming pulse of phytodetritus can clear out water layers of 7 – 8 mg/L (Thomsen & McCave, 2000; Hill and Nowell, 1990). Since the NORI site is located at the eastern part of the CCZ (vanReusel et al., 2016), pulses of organic rich phytodetritus can be expected and this would have an impact even on such comparably low particle concentrations of 7 - 8 mg/l, which are still 1-2 orders of magnitude higher than the background value for the Pacific. It is therefore recommended to estimate the newly formed background concentration of fine particles in suspension which will disperse in the Pacific Ocean after large scale midwater injection from mining operations has started. The background values will slowly increase over time (1 – 20 years of operations). However, if the modeling of DHI shows very low particle concentrations of ≈ 100 µg/L for the far field site around an injection point and this can be verified during onsite experiments, I would not expect a significant impact on the vertical migration behavior of zooplankton. One can however expect that research institutions, NGOs and the ISA will be very skeptical towards these modeling results, especially since recent discussions between ISA, potential contractors and the science community favor the reinjection of the return flow behind the collector. This however could dilute the concentrated plume behind the collector. One contractor claims to invent an additional concentrator, which produces nodule sized sediment pellets. I have however not seen any evidence for that. It is also important to point out that even under a turbulence of 10 G, a plume of 0.5 g/L produces aggregates of at least 600 µm in size within the first 10-15 minutes (Gillard et al., 2019, Fig. 3).

E. Effective settling velocities [w_s] of populations of plume aggregates in the water column simulator: settling inside a developing fluid-mud layer, typically expected behind the collector

While the above mentioned results are normally used for numerical modeling of plume dispersal, we also applied another approach to better understand the behavior of concentrated plume injections $\geq 1\text{g/L}$ in the BBL near the seafloor for comparison. For that we used the data from the Aqualogger turbidity meter, which automatically adapts to increasing particle concentrations. The calculated settling velocities presented below describe the behavior of a floc population. Theory (after Dankers & Winterwerp, 2007): the single floc settling in still water (see table 1) has a specific settling velocity, which is a function of its shape, size, density and the viscosity of the fluid. When the concentration of particles increases, they start to interfere and hinder each other, thereby reducing their settling velocity (see also video). This is called hindered settling and the settling velocity is referred to as the effective settling velocity. When the concentration increases further, the particles tend to be in constant contact with each other, and a particle framework builds up. The change from a water supporting system to a sediment supporting system is called gelling when early consolidation starts.

W_s at 1 g/L

The effective settling velocities of the floc population was calculated via the particle concentrations from the vertical profiles in the water column simulator and from single point measurements at 50 cm water depth. The initial settling velocities of the fast growing aggregates during the first 10 minutes after the plume was released was ≈ 0.1 cm/sec (86.4 m/day). Between 10 min and 30 min when hindered settling began, w_s was reduced to 0.03 cm/s (28.8 m/day). During the export phase 2 (see fig.7) w_s ranged between 0.01-0.02 cm/s (7.2 – 14.4 m/day). After 60 minutes > 90 % of the fallout has already occurred and all large aggregates had settled with $w_s > 0.02$ cm/s (> 14.4 m/day), Table 2A. Interestingly, the settling velocities determined via the water column simulator were significantly lower than those measured in the settling column. They represent the w_s of the floc population and not of individual aggregates, and the settling occurred under low turbulence of 0.1 G while the data on w_s in table 1 result from measurements in stagnant water of the settling column.

Table 2A, 1g/L

Part.Conc [mg/L]	Minutes	w_s [cm/s]	w_s [m/h]	Settling velocity [m/day]
1165	0			
905	10	0.1	3.6	86.4
418	30	0.03	1.2	28.8
140	60	0.02	0.6	14.4
72	120	0.01	0.3	7.2
46	240	0.01	0.3	7.2

 W_s at 10 g/L

The effective settling velocities of these flocs decreased from 0.1 cm/s during the first 30 minutes to 0.02 cm/s after 60 minutes when > 90 % of the fallout has occurred. These significantly lower settling velocities during the first 30 minutes are the result of hindered settling which definitely also occurred right above and within the thickening mud layer and resulted in a further reduction of the settling velocities of the incoming aggregates to 0.006 cm/s, Table 2B. The difference between W_s measured in the settling column and via water column simulator is even more pronounced at 10 g/L. Settling velocities per day are almost two orders of magnitude lower during the first 60 minutes. The data in table 2 represent the settling behavior of groups of flocs (floc population) and not individual ones (Table 1) and were determined under turbulent flow of 1 G (15 cm/s flow velocity). These results should give DG a first insight, how the plume is dispersed and settles under high concentrations in fluid mud and numerical modeling of sediment transport should take this into account. Videos are provided from these experiments for discussion with your modeler team.

Table 2B, 10 g/L

Part.Conc [mg/L]	Minutes	w_s [cm/s]	w_s [m/h]	Settling velocity [m/day]
10170	0			
7033	30	0.01	0.4	9.6
770	60	0.02	0.6	14.4
80	120	0.01	0.4	9.8
60	180	0.01	0.3	6.8
50	240	0.006	0.2	5.2

Comparing the size and settling velocities of aggregates under the two different initial plume concentrations

reveals that higher concentrations of 10 g/L result in larger floc size but these populations of larger flocs settle with lower settling velocities under conditions of hindered settling and turbulent flow. At 1 g/L plume concentration under normal deep sea flow conditions of 0.1 G (≈ 4 cm/s), the settling velocities determined in the water column simulator under low turbulence of 0.1 G during the initial phase of aggregation are at least more comparable to those from the stagnant settling tube for similar d_{50} values (see table 1, d_{50} after 10 and 180 minutes); however it strongly deviates from conditions of elevated plume concentrations (10 g/L) and elevated turbulence (1G). The lower settling velocities of larger flocs during the core phase of aggregation at 10 g/L is a combination of both, hindered settling and elevated turbulence. Hindered settling starts when large flocs at high concentrations hinder each other in settling (see 400 MB video of 10 g at T30, provided in September or on demand). In the video, large aggregates are visible which constantly form larger or smaller units after they get in contact with others and are clearly hindered in settling). This behavior is known from studies in sediment transport and stated to start at concentrations between 1 to 15 g/L. Increasing turbulence is also expected to keep the flocs in suspension for longer periods and decrease the averaged settling speed of a floc population, especially when compared to results from stagnant settling columns (Tran et al., 2018). We are offering support to your modelers and AllSeas for potential recommendations on how to handle the collector exhaust pipe in order to influence a forming mud layer.

Similar effective settling velocities of 0.01 – 0.02 cm/s for floc populations have also been experimentally determined by Dankers & Winterwerb (2007) for highly concentrated mud suspensions under hindered settling (called settling suspensions in hindered settling regimes). Table 3 summarizes the settling (fallout) times for floc populations using the results from the water column simulator. During the first 120 minutes (data from 30, 60, 120 minutes) of deposition averaged values of a w_s of 0.02 cm/s for 1 g/L at 0.1 G and 0.013 cm/s for 10g/L at 1 G (both using data from table 2) **are used for the fluid mud layer which rapidly develops**. It is important to note that hindered settling under plume concentrations of both 1g/L and 10 g/L consequently results in extended travel times which carry the plume particles over larger distances away from the injection point. If we assume a plume injection of 1 g/L under low flow conditions of 0.1 G at a height of 10 m above the sea floor (Table 3, [1]) and an export phase with settling velocities of ≈ 0.02 cm/s for the floc population in the fluid mud it would take approximately 14 hours for a > 90% fallout through the full 10 m water column. These particles would travel over distances of 1.8 km. Extended distances of 7.5 km would occur under the flow velocities of 1 G (15 cm/s; deep sea eddy). Increasing concentrations in the mud-layer would also lead to gelling and subsequently lower settling velocities. It is important to note that dispersal via turbulence would increase the settling velocities again, when aggregates switch from hindered settling to individual settling; and the formation of a density currents **could drastically speed up the horizontal export velocity**. The fluid-mud would then be exported along a slope or through a gulley into a depression on the seafloor, possibly kilometers away. **If the area B on figure 21 (p.28) shows such an area of seafloor depression (valley, M.Clarke, pers.comm.), we would recommend to start modeling gravity plumes for a harvesting site north of that area for use as potential plume dump site.**

Table 3. Time for the fallout of 90 % of the plume particles under 0.1G and 1G conditions from different plume injection heights into a fluid mud layer assuming an average fallout velocity of A: 0.02 cm/s (1 g/L scenario) and B: 0.013 cm/s (10 g/L scenario) and that such fluid mud layers have a maximum height of 10 m.

A: w_s of 0.02 cm/s	Minutes to settle	Hours to settle	Days to settle	Travel distance (km) at 0.1 G	Travel distance (km) at 1 G
1 m	83	1.4	0.1	0.2	0.8
5 m	417	6.9	0.3	0.9	3.8
10 m [1]	833	13.9	0.6	1.8	7.5

B: Ws of 0.013 cm/s	Minutes to settle	Hours to settle	Days to settle	Travel distance (km) at 0.1 G	Travel distance (km) at 1 G
1 m	128	2.1	0.1	0.3	1.2
5 m	641	10.7	0.4	1.3	5.8
10 m [2]	1282	21.4	0.9	2.7	11.5

Under scenario B in table 3 (10 g/L, [2]) it would take 21.4 hours for a 90% fallout through the full 10 m water column. Under these flow conditions particles would travel over distance of 2.7 - 11.5 km.

Settling within the mud layer

Aggregates formed under elevated plume concentrations develop a different settling behavior and cannot be described via individual aggregates but rather as a floc population (see 2.2 Aggregation dynamics). The sedimentation under 10 g/L in a 1 m water column or 1 g/L in a 10 m water column cause the formation of a fluid mud layer with concentrations rapidly exceeding 30 g/L (Fig.8, III). The settling velocity of the floc population within the mud layer was strongly decreased and can be estimated by measurements of the compaction of this layer. Fig 12 shows the rapid sedimentation of aggregates under different particle concentrations during the flume experiments in a 16 cm high waterlayer above Type 1 nodules (Scenario 3-5). Within the first 5-10 minutes the sedimentation of the aggregating plume particles is characterized by rapid decrease in particle concentrations (see also Figures 7, 8 for 1 m) within the water layers above the Type 1 nodules in the seawater flume (Fig. 12). The much shorter clear-out time is the result of the lower water column (16 cm vs. 100 cm of the water column simulator). As shown in fig. 13 (scenario 3, 5 minutes after release), a mud layer is formed during these first minutes which can be characterized by an initial loose layer of incoming aggregates, which rapidly gets compacted by 75 % once the incoming aggregate flux diminishes (Fig 12, 13, scenario 3, after 10 min). After that, further compaction and consolidation of the newly formed mud layer is below 10 %. This change from a water supporting fluid mud system to a sediment supporting system is called gelling when early consolidation took place.

This mud layer would remain loose for hours or days at its top section and increasingly consolidated in the lower section until the incoming flux of aggregates has diminished. Figures 25 and 26 on page 26/27 show such a loose mud layer above the test section of the Type 1 nodules and in the water column simulator.

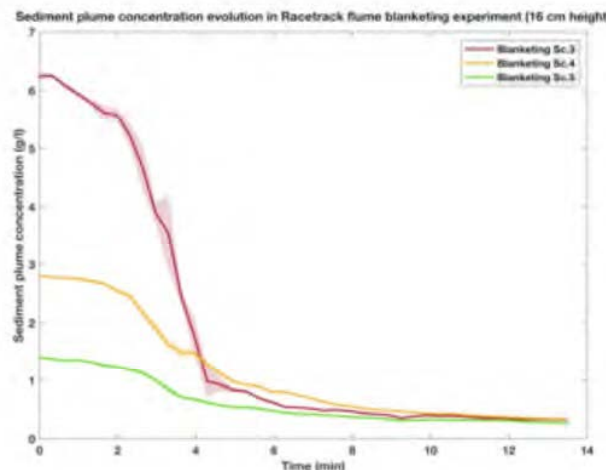


Fig. 12. Plume concentration (aggregation) during the first 15 minutes after release in three scenarios Sc.3: 1 g/L, Sc.4: 0.5 g/L, Sc.5: 0.25 g/L to simulate conditions in a 1 m water column.